Article

Application of Turkevich Method for Gold Nanoparticles Synthesis to Fabrication of SiO$_2$@Au and TiO$_2$@Au Core-Shell Nanostructures

Paulina Dobrowolska [1], Aleksandra Krajewska [1], Magdalena Gajda-Rączka [1], Bartosz Bartosewicz [1], Piotr Nyga [1] and Bartłomiej J. Jankiewicz [1,*]

Institute of Optoelectronics, Military University of Technology, Warsaw 00-908, Poland;
E-Mails: paulina.doborowolska@student.wat.edu.pl (P.D.); aleksandra.krajewska@wat.edu.pl (A.K.);
magdalena.gajda-raczka@wat.edu.pl (M.G.R.); bartosz.bartosewicz@wat.edu.pl (B.B.);
piotr.nyga@wat.edu.pl (P.N.)

* Author to whom correspondence should be addressed; E-Mail: bartlomiej.jankiewicz@wat.edu.pl;
Tel.: +48-261-839-981; Fax: +48-22-666-8950.

Academic Editor: Gururaj V. Naik

Abstract: The Turkevich synthesis method of Au nanoparticles (AuNPs) was adopted for direct fabrication of SiO$_2$@Au and TiO$_2$@Au core-shell nanostructures. In this method, chloroauric acid was reduced with trisodium citrate in the presence of amine-functionalized silica or titania submicroparticles. Core-shells obtained in this way were compared to structures fabricated by mixing of Turkevich AuNPs with amine-functionalized silica or titania submicroparticles. It was found that by modification of reaction conditions of the first method, such as temperature and concentration of reagents, control over gold coverage on silicon dioxide particles has been achieved. Described method under certain conditions allows fabrication of semicontinuous gold films on the surface of silicon dioxide particles. To the best of our knowledge, this is the first report describing use of Turkevich method to direct fabrication of TiO$_2$@Au core-shell nanostructures.

1. Introduction

In recent years, nanotechnology is one of the fastest growing fields in science and engineering. One of the results of extremely rapid progress in this field is the discovery of the large number of functional materials in which at least one dimension is in the range of 1 to 100 nm. Some of the most prominent examples of these materials are noble metal nanostructures, such as nanoparticles (NPs) [1], nanowires [2,3], nanorods [3–5], nanotriangles [6], nanostars [7] and many others. Various properties and thus also possible applications of noble metal nanostructures, are dependent on their composition, shape and size [8–10]. The noble metals were also used for fabrication of more complex hybrid nanostructures, where they are combined with other materials. This often results in new functionalities as compared to nanostructures made from noble metal only. The core-shell nanostructures consisting of oxide core and noble metal shell is an interesting example of such hybrid nanostructures.

The core-shell nanostructures have received increasing attention since Halas and co-workers [11] reported studies on the synthesis of SiO_2@Au nanoparticles. In this work, a continuous gold nanoshell was grown on the surface of amine-functionalized silica in a two-step process. The amine-functionalized silica particles were decorated with very small Au nanoparticles (1–2 nm in diameter) in the first step. In the next step, the growth of the shell on gold-decorated silica particles was realized by a subsequent reduction of an aged mixture of chloroauric acid and potassium carbonate by a solution of sodium borohydride. The Au nanoparticles on silica surface served as a nucleation sites for the reduction. One of the most important characteristics of the core-shell nanostructures is that their optical properties, localized surface plasmon resonance (LSPR) band positions, can be tuned by their geometry, core radius/shell thickness ratio. The possibility of core-shell nanostructures optical properties tuning has opened the door to many applications such as cancer therapy [12], surface enhanced spectroscopies [13,14] or steam generation for solar autoclave [15].

Following work of Halas [11], several approaches to fabrication of core-shell nanostructures based on the silica core and gold shell have been reported [16–33]. The most commonly used approach to synthesis of core-shell nanostructures based on silica and gold involves a two-step process, deposition of gold seeds on functionalized silica surface, followed by gold shell growth. Research studies based on this approach were mainly focused on the investigations of the influence of silica surface functionalization and reducing agent used for shell growth on the formation of gold shell.

The silica surface functionalization is crucial for deposition of small gold nanoparticles, which serve as seeds for shell growth. The surface of silica was most frequently functionalized with various organosilanes containing functional groups with high affinity to gold, such as amino ($-NH_2$) or mercapto (-SH) group [11,17], or using polymers containing multiple $-NH_2$ groups, such as polyethyleneimine (PEI) [18] or poly(diallyldimethylammonium chloride) (PDADMAC) [19]. In most cases, the organosilanes-containing amino group were used for functionalization because they provided uniform and relatively high surface coverage (up to 30%) with gold nanoparticles, which is very important for obtaining smooth continuous shell.

Most of the studies regarding a two-step process focused on the influence of the gold salts reducing agents on the shell formation. In the first studies on synthesis of silica-gold core-shell nanostructures, sodium borohydride was used as a reducing agent [11], however one of the most often used reducing agent in SiO_2@Au nanostructures synthesis is formaldehyde [20–22]. Due to the toxicity of

formaldehyde, researchers have also looked for safer alternatives to it, such as glucose [23] or ascorbic acid [24]. Also, hydroxylamine [25] and CO [26] were used as reducing agents. Use of gaseous CO as reducing agent results in uniform shell formation [26].

Only a few studies regarding direct growth of gold shell on the non-functionalized silica surface have been reported. These studies include the reduction of gold (I) chloride in acetonitrile with ascorbic acid [27], formaldehyde stimulated shell growth on Sn-seeded silica particles [28] and ultrasound assisted deposition of gold nanoparticles on silica particles surface [29]. Similarly, studies on direct growth of gold shell on amino-functionalized silica particle are limited to a few articles. For example, gold salts were directly reduced on functionalized surface of SiO_2 particles using formaldehyde [30]. An interesting approach involves direct growth of gold shell on functionalized silica surface by reduction of gold salts with trisodium citrate [31–33]. Trisodium citrate was used by Turkevich [34] and Frens [35] for the synthesis of monodispersed gold nanoparticles and has become probably one of the most often used reducing agents for this purpose. It is not surprising since it is cheap, not hazardous, by varying its concentration one can control the size of synthesized gold nanoparticles, and, most importantly, it acts as both reducing agent and stabilizing agent. In studies reported by Zhang *et al.* [31], gold salts were reduced directly on the surface of amino-functionalized silica particles (average diameter of 227 nm) and the silica particles decorated with gold particles (average diameter of 14 nm) at 100 °C by rapidly injected trisodium citrate. In both cases rather non-uniform coverage with gold was achieved, however the coverage was higher in case of reduction on silica particles decorated with gold nanoparticles. Storti *et al.* [32] synthesized SiO_2@Au core-shell nanoparticles by gold salts reduction on amino-functionalized silica nanoparticles (average diameter 16 nm) obtained in a one-step process. The formation of complete gold shell in these studies was carried out by slow addition of $HAuCl_4$ solution to silica particles suspension containing trisodium citrate at 100 °C [32]. In studies of Zhang *et al.* [33], gold shell was grown on the tris(2,2′-bipyridyl)ruthenium(II) chloride embedded amino-functionalized SiO_2 particles (diameter ~70nm). In this method, reducing agent was added dropwise to mixture containing functionalized cores and gold salt. Au shells of different thickness were obtained by adjusting the ratio of the SiO_2 NPs and gold salt, while maintaining trisodium citrate in excess.

Herein, we report studies on the application of modified Turkevich synthesis method of Au nanoparticles to direct fabrication of SiO_2@Au core-shell nanostructures. The effect of reaction temperature and amount of silica particles used in the reaction on deposition of gold nanostructures on the amino-functionalized silica particle was investigated. In addition, this method was for the first time applied to synthesis of TiO_2@Au core-shell nanostructures.

2. Results and Discussion

The synthesis of SiO_2@Au and TiO_2@Au core-shell nanostructures described in this article was carried out according to procedures shown in Figure 1. The commercially available submicrometer silica and titania (rutile) particles, which are used as cores, were functionalized with $-NH_2$ groups. The amino groups served as anchor groups, which bind gold nanoparticles to surface of functionalized SiO_2 and TiO_2 particles. In the first method used in these studies, amino-functionalized cores were decorated with 16–20 nm AuNPs synthesized using Turkevich method [34]. These particles served as

reference structures to nanostructures obtained by direct reduction of gold salts on functionalized core using modification of Turkevich method. The syntheses of SiO₂@Au and TiO₂@Au nanostructures via direct reduction were carried out at different temperatures. In addition, the influence of different amounts of silica cores on the morphology of gold shell was investigated.
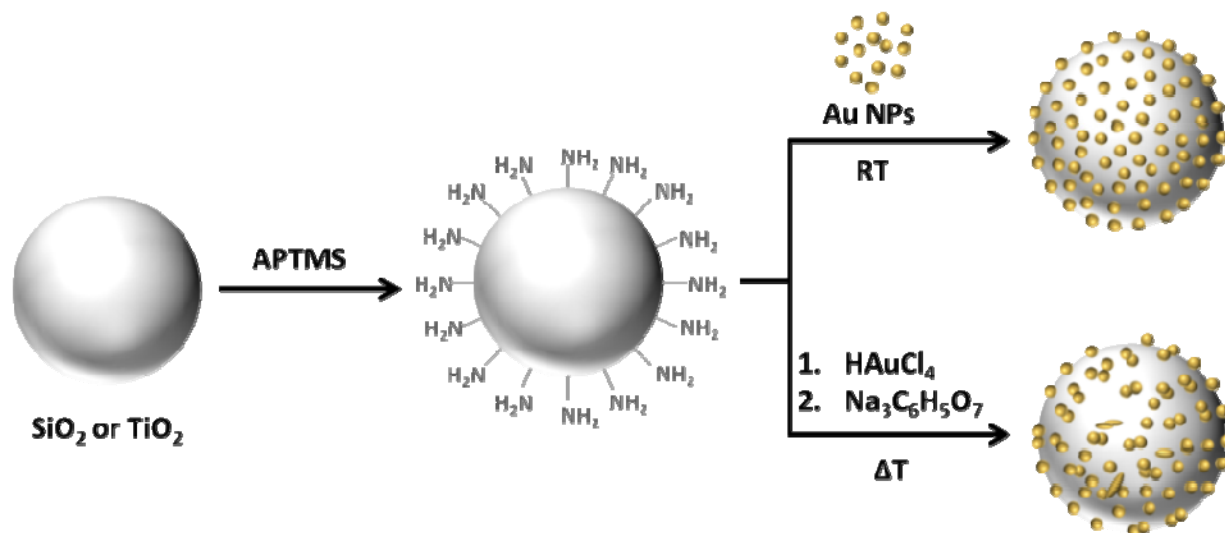

Figure 1. Schematic illustration of SiO₂@Au and TiO₂@Au core-shell nanostructures fabrication via decoration of NH₂-functionalized cores with AuNPs and via direct reduction of gold salts.

2.1. Deposition of AuNPs on Nh2-Functionalized Silicon Dioxide and Titanium Dioxide Cores

The silicon dioxide and titanium dioxide cores shown in Figure 2a,c were functionalized with amino groups and mixed with Turkevich AuNPs to yield structures shown in Figure 2b,d. For both core materials, the deposition yields structures with monodispersed gold nanoparticles evenly distributed on the surface of SiO₂ and TiO₂ cores. Gold nanoparticles are usually well separated on the SiO₂ core surface, however in some areas of core surface clusters containing from two up to several AuNPs are also observed. This phenomenon is more pronounced in the case of TiO₂ cores, where AuNPs are more densely packed. The degree of surface coverage with AuNPs and the way AuNPs are distributed on the core surface are dependent on the surface modifier used for core surface functionalization [36] and can be controlled by amount of AuNPs used for this process.
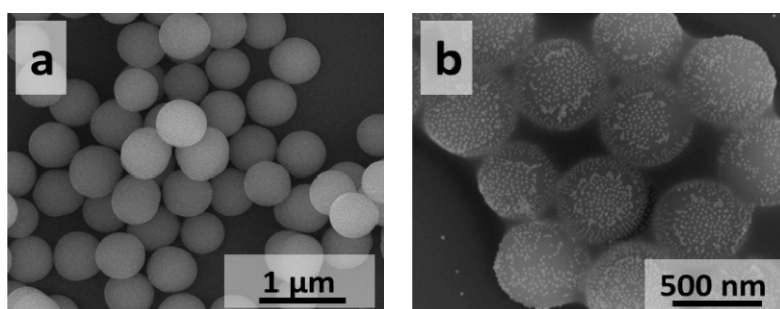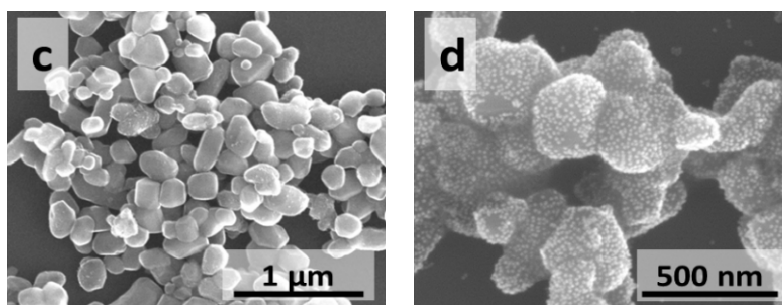

Figure 2. *Cont.*

Figure 2. Scanning Electron Microscopy (SEM) images of silicon dioxide and titanium dioxide cores before and after deposition of Turkevich AuNPs: (**a**,**b**) SiO_2 and (**c**,**d**) TiO_2.

Different gold coverage on the SiO_2 and TiO_2 cores may be associated with the different content of OH groups on the surface of non-functionalized SiO_2 and TiO_2 cores, which may be up to four times higher for TiO_2 [37–39]. The higher number of OH groups on the surface of TiO_2 particles may result in higher number of NH_2 groups after functionalization step and thus provide more anchoring groups for AuNPs binding.

The UV-Vis spectra of silicon dioxide and titanium dioxide cores before and after deposition of Turkevich AuNPs are shown in Figure 3. Due to separation of AuNPs on the surface of silica cores, UV-Vis spectrum of SiO_2@Au nanostructures closely resembles spectrum of AuNPs (not presented) and has extinction band centered at about 550 nm. The significant red shift of the maximum of absorption (λ_{max} = 670 nm) was observed in case of TiO_2@Au nanostructures. The spectral location of plasmon resonance of single gold nanoparticle is dependent on the refractive index of surrounding medium. Therefore, the red shift observed for TiO_2@Au in the UV-Vis spectrum as compared to SiO_2@Au is likely related to the higher refractive index of TiO_2 (n ~ 2.2–2.6) particles compared to SiO_2 particles (n ~ 1.45). In addition, both red shift and broadening of the spectrum may be associated with dense packing of AuNPs on TiO_2 particles surface resulting in Au nanoparticles plasmon-plasmon coupling.
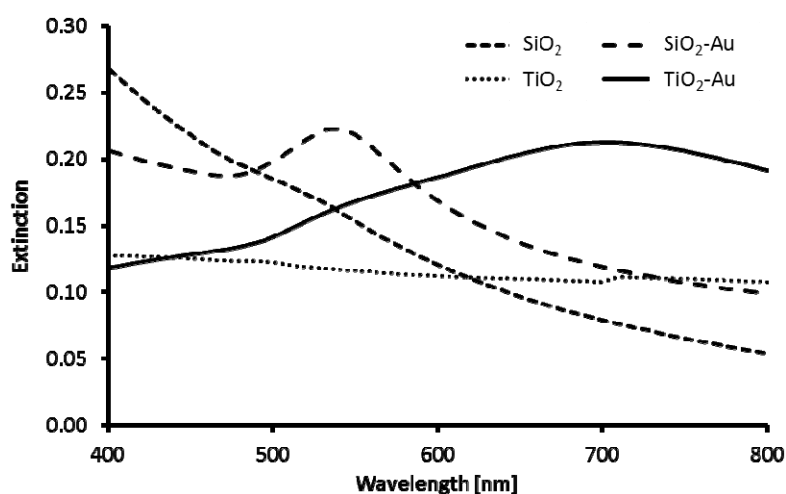

Figure 3. UV-Vis spectra of silicon dioxide and titanium dioxide cores before and after deposition of Turkevich AuNPs.

2.2. Direct Reduction of Gold Salts on NH₂-Functionalized Silicon Dioxide Cores

The SiO$_2$@Au nanostructures obtained by direct reduction of gold salts on functionalized SiO$_2$ particles at temperatures in the 50–100 °C range are shown in Figure 4. For all temperatures, in addition to desired core-shell structures, formation of large amount of gold nanoparticles not attached to SiO$_2$ particles was observed. The aim of lowering the reaction temperature was to slow down gold salts reduction process and therefore to provide more time for gold seeds to bind to NH$_2$-functionalized silicon dioxide cores. As a result, higher coverage of cores with gold was expected. However, the opposite effect was observed. Denser and more uniform coverage was observed for higher reaction temperatures 80–100 °C. In these temperatures, syntheses were more reproducible. Direct reduction of gold salts on SiO$_2$ cores at higher temperatures yields SiO$_2$@Au nanostructures with denser coverage of gold as compared to SiO$_2$@Au nanostructures obtained by AuNPs deposition. In addition, the gold nanostructures fabricated on core surface by direct reduction are of different shape and sizes, ranging from a few to several nanometers. Despite the fact that variety of gold nanostructures were obtained on SiO$_2$ cores, their UV-Vis spectra are very similar to the UV-Vis spectrum of silica cores decorated with AuNPs (Figures 3 and 5).
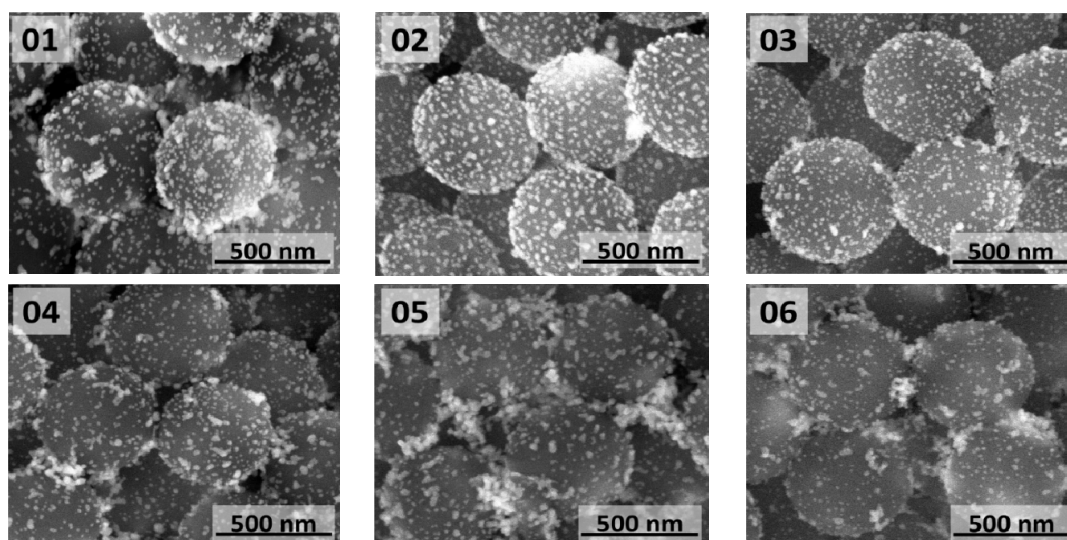

Figure 4. SEM images of SiO$_2$@Au nanostructures obtained by direct reduction of gold salts on functionalized SiO$_2$ particles at various temperatures: (**01**) 100 °C; (**02**) 90 °C; (**03**) 80 °C; (**04**) 70 °C; (**05**) 60 °C; and (**06**) 50 °C.

The SiO$_2$@Au nanostructures obtained by direct reduction of gold salts at 90 °C and 100 °C in reaction mixture containing different amounts of functionalized SiO$_2$ particles (2.5, 13, 50 and 125 µg per mL of reaction mixture) are shown in Figure 6. These core-shell nanostructures could also be compared to SiO$_2$@Au nanostructure shown in Figure 4 (02). The highest coverage of core surface was obtained when only 2.5 µg/mL of silica core particles were used (Figure 6 (07)). In these conditions, semicontinuous gold film formed on the silica surface. Unfortunately, due to low number of used silica cores, it was impossible to measure UV-Vis spectra of these structures. Structures with such shell morphology are expected to have high extinction in broad spectral range extending to longer wavelengths [40,41]. Based on SEM images (Figure 6), it is clearly seen that by increasing number of

functionalized cores, lower gold coverage is achieved and also less Au particles and larger separation between them are observed. The UV-Vis spectra of (08)–(10) are qualitatively the same as for the (03)–(04) samples, but with less pronounced AuNPs extinction peak.
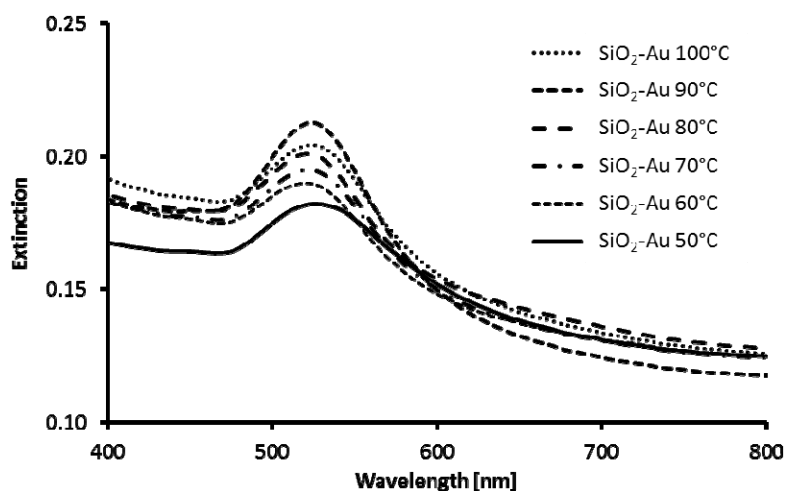

Figure 5. UV-Vis spectra of SiO_2@Au nanostructures obtained by direct reduction of gold salts on functionalized SiO_2 particles at various temperatures: (**01**) 100 °C; (**02**) 90 °C; (**03**) 80 °C; (**04**) 70 °C; (**05**) 60 °C; and (**06**) 50 °C.
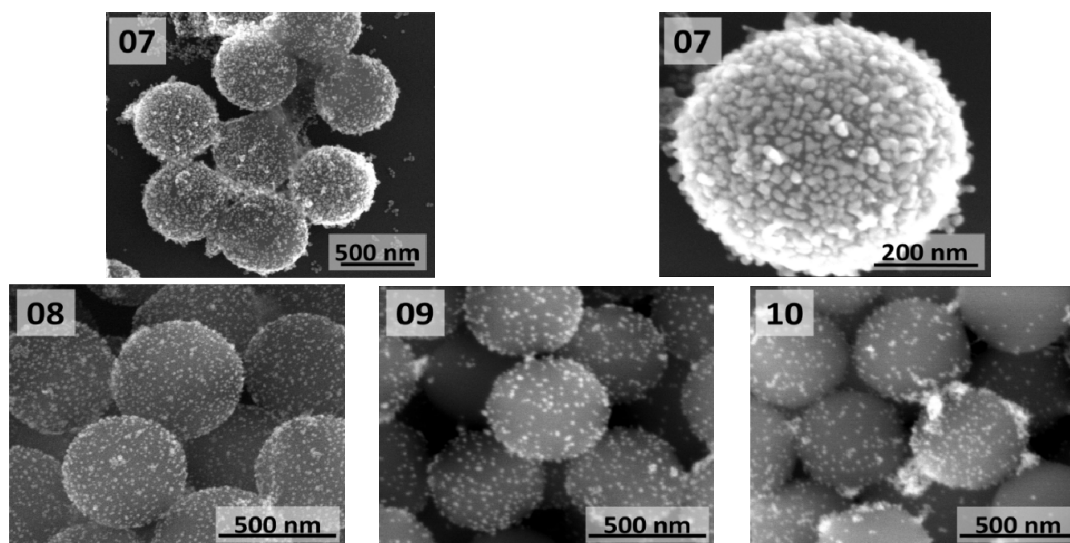

Figure 6. SEM images of SiO_2@Au nanostructures obtained by direct reduction of gold salts in reaction mixture containing different amounts of functionalized SiO_2 particles: (**07**) 2.5 µg/mL; (**08**) 13 µg/mL; (**09**) 50 µg/mL; and (**10**) 125 µg/mL.

The comparison of the results obtained in these studies, syntheses (1)–(10), to previously reported studies [31–33] on SiO_2@Au fabrication using trisodium citrate as reducing agent of gold salts yields some interesting observations. The method described by *Zhang et al.* [31], which closely resembles method reported in this article, yields SiO_2@Au nanostructure with rather low surface coverage with gold, even in case of deposition of AuNPs on functionalized cores. In the studies reported here, surface coverage seems to be higher. These differences could be associated with the methods used for the

functionalization of silica core. In our studies, functionalization of core surfaces in toluene allowed obtaining higher coverage with gold nanoparticles than in the case of functionalization in ethanol used in Zhang studies. It is quite difficult to relate the here reported studies to earlier studies [31–33] where trisodium citrate was used as a reducing agent. For all three cases, cores of different sizes, different silica surface functionalization methods, and reaction conditions were used.

2.3. Direct Reduction of Gold Salts on NH2-Functionalized Titanium Dioxide Cores

The TiO2@Au nanostructures obtained by direct reduction of gold salts on functionalized TiO2 particles using trisodium citrate at temperatures in the 50–100 °C range are presented in Figure 7. To the best of our knowledge, it is the first time this method is used for synthesis of TiO2@Au nanostructures. In our studies on the synthesis of TiO2@Au core-shell structures, we have applied many methods that were used for SiO2@Au [16]. However, in many cases methods, which worked fine for SiO2 failed for TiO2. It is related to the fact that opposite to chemically inert SiO2, TiO2 exhibits photocatalytic properties even in amorphous form. Because of that, formaldehyde, most commonly used reducing agent in case of SiO2, did not work in our experiments for TiO2. From the other hand, as shown in studies reported here, use of trisodium citrate yields TiO2@Au core-shell structures with relatively high gold coverage.

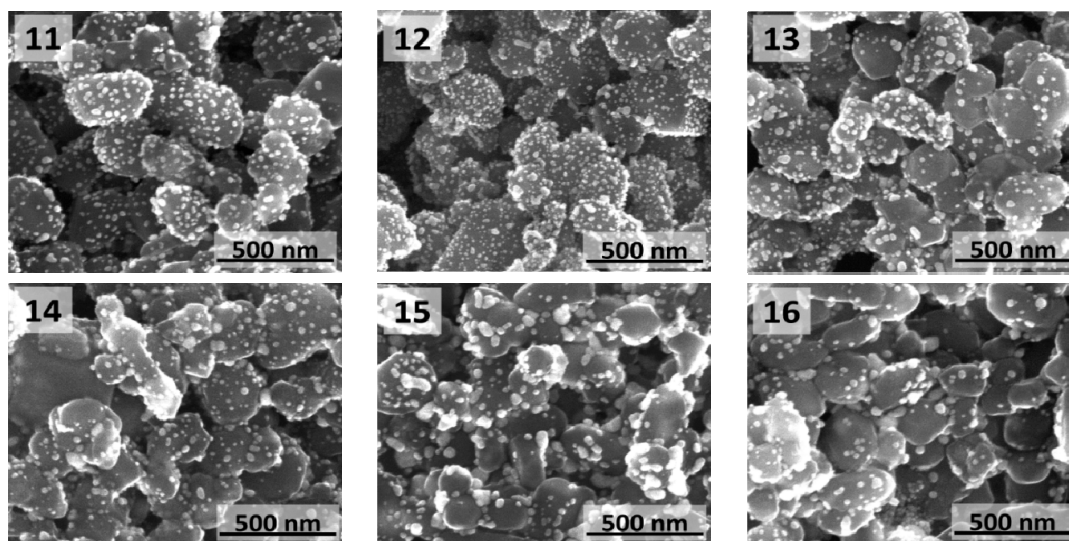**Figure 7.** SEM images of TiO2@Au nanostructures obtained by direct reduction of gold salts on functionalized TiO2 particles at various temperatures: (**11**) 100 °C; (**12**) 90 °C; (**13**) 80 °C; (**14**) 70 °C; (**15**) 60 °C; and (**16**) 50 °C.

Similarly to studies for silica cores, the aim of lowering temperature was to slow down gold salts reduction process and therefore provide more time for gold seeds to bind to NH2-functionalized titanium dioxide cores. As a result, higher coverage of cores with gold was expected. However, it was observed that by lowering reaction temperature, less gold nanostructures were formed on the surface of TiO2 cores and, in addition, the size of AuNPs increased as the temperature was lowered. Lower number of gold nanostructures attached to cores observed for lower temperature reactions may be related to unbinding of large gold nanostructures from the core surface during the work up of a

reaction. It seems that denser surface coverage with gold was observed when AuNPs were deposited on the NH_2-functionalized titanium dioxide cores (Figure 2d).

The UV-Vis spectra of TiO_2@Au nanostructures obtained by direct reduction (10–15) (Figure 8) correspond well to spectrum of AuNPs and differ significantly from spectra of TiO_2 cores decorated with AuNPs (Figure 3). In all cases, small red shifts of absorption maximum (λ_{max}) as compared to spectrum of AuNPs are observed, which is likely caused by larger size of gold nanostructures on the TiO_2 surface compared to Turkevich AuNPs and TiO_2 refractive index being higher than that of water.
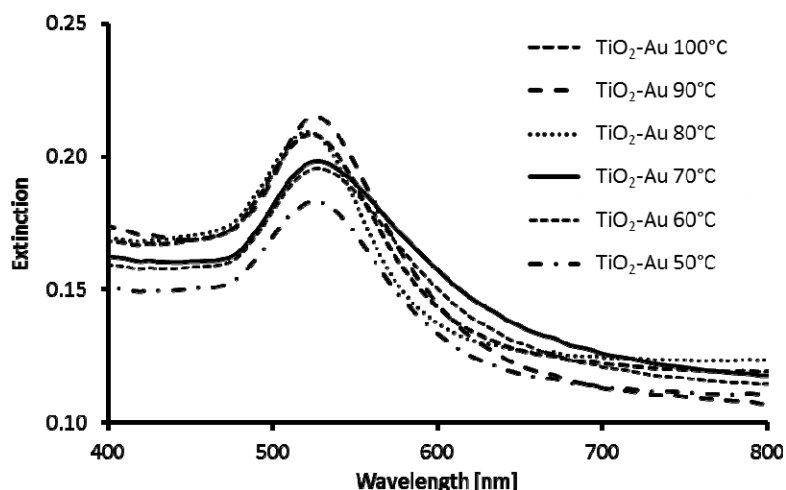

Figure 8. UV-Vis spectra of TiO_2@Au nanostructures obtained by direct reduction of gold salts on functionalized TiO_2 particles at various temperatures: (**11**) 100 °C; (**12**) 90 °C; (**13**) 80 °C; (**14**) 70 °C; (**15**) 60 °C; and (**16**) 50 °C.

3. Experimental Section

3.1. Reagents

Silica particles (spherical particles with average diameter of 670 nm), titania particles (rutile particles of irregular shape and size in range of 100–200 nm) and trisodium citrate were purchased from POCH S.A. (3-Aminopropyl)-trimethoxysilane (APTMS) was purchased from Sigma Aldrich. Hydrogen tetrachloroaurate(III) trihydrate ($HAuCl_4$) was purchased from Alfa Aesar and was used to prepare 5% dark-aged stock solution of chloroauric acid, later used in the experiments. Other reagents were of analytical grade. All the chemicals were used without further purification. Deionized (DI) water (resistance > 18.2 MΩ) used in all synthesis and washing was prepared by an ultrapure water system HLP 5UV (Hydrolab).

3.2. Functionalization of Silica and Titania Submicroparticles

Silica and titania submicroparticles were functionalized with amine groups using modified method described by Jaroniec *et al.* [17]. The silica or titania particles (0.5 g) were added to 50 mL of anhydrous toluene in Falcon tube, which was then placed in ultrasonic bath and sonicated for 1 h. The suspension was transferred to round bottom flask and allowed to stir vigorously for 1 h. Next, the 2.5 mL of APTMS was added to mixing suspension. Such reaction mixture was boiled under reflux for 24 h.

After completion of the reaction, modified particles were washed several times on a membrane filter with small portions of toluene and ethanol to remove an excessive amount of modifier. The functionalized particles were dried overnight in an oven at ~100 °C.

3.3. Deposition of Turkevich AuNPs on Silica and Titania Particles

Gold nanoparticles were synthesized according to Turkevich method [34]. Briefly, 1 mL of solution of 5 mM $HAuCl_4$ in DI water was added to 18 mL of DI water and mixture was heated until it began to boil. One milliliter of 0.5% trisodium citrate solution was added as soon as boiling commenced. The reaction mixture was heated until evident color change had occurred and then it was removed from heating plate and stirred until it cooled down to room temperature.

Five milligrams of amine-functionalized silica or titania particles were dispersed in 10 mL of DI water under ultrasound for 1 h. Next, 4.5 mL of the silica or titania functionalized particles suspension was added to 30 mL of Turkevich AuNPs solution and mixed for a few hours. In order to remove AuNPs unattached to silica or titania particles surface, the reaction mixture was subjected to a few washing steps by centrifugation and redispersion in 0.5% solution of trisodium citrate.

3.4. Direct Deposition of Au Nanostructures on Silica and Titania Particles Using Turkevich Method

In typical synthesis, 1 mL of 5 mM $HAuCl_4$ aqueous solution was added to 17 mL of DI water and mixed for 5 min before addition of 1 mL of water suspension containing 0.5 mg of amine-functionalized silica or titania particles. Resulting reaction mixture was heated until it reached the selected reaction temperature in the 50–100 °C range and then the preheated 1 mL of 0.5% trisodium citrate solution was added. The reaction mixture was heated until evident color change had occurred and then it was removed from heating plate and continued to stir until it cooled down to room temperature. In order to remove AuNPs unattached to silica or titania particles surface the reaction mixture was subjected to a few washing steps by centrifugation and redispersion in 0.5% solution of trisodium citrate. Conditions of (01)–(16) syntheses described in article are given in Tables 1 and 2.

Table 1. Reaction temperatures and amount of SiO_2-NH_2 particles used in the syntheses 01–10.

Sample Reaction Conditions	01	02	03	04	05	06	07	08	09	10
SiO_2-NH_2 (µg/mL)	25	25	25	25	25	25	2.5	13	50	125
T (°C)	100	90	80	70	60	50	100	90	90	90

Table 2. Reaction temperatures and amount of TiO_2-NH_2 particles used in the syntheses 11–16.

Sample Reaction Conditions	11	12	13	14	15	16
TiO_2-NH_2 (µg/mL)	25	25	25	25	25	25
T (°C)	100	90	80	70	60	50

3.5. Characterization

The UV–Vis extinction spectra were measured at room temperature using Lambda 900 UV-Vis-NIR spectrophotometer (Perkin Elmer, Waltham, MA, USA) in the 400–800 nm spectral range. Suspensions of synthesized nanostructures were measured in 1 cm optical path quartz cuvette.

The morphology of SiO$_2$-Au and TiO$_2$-Au nanostructures was characterized based on the images obtained using a Quanta 3D FEG Dual Beam scanning electron microscope (FEI, Hillsboro, OR, USA). Samples for SEM were prepared by drop-casting of suspensions of core-shell nanostructures on silicon wafer and drying in air.

4. Conclusions

In this paper, we applied Turkevich method for AuNPs synthesis to fabrication of SiO$_2$@Au and TiO$_2$@Au nanostructures. The nanostructures synthesized using this method were compared to SiO$_2$@Au and TiO$_2$@Au nanostructures obtained by deposition of Turkevich AuNPs on amino-functionalized SiO$_2$ and TiO$_2$ cores. The nanostructures fabricated using both methods have different morphologies of gold shell and exhibit different optical properties. In the case of SiO$_2$ cores, both methods may yield core-shell structures with similar optical properties. However, by control of reaction conditions, it is possible to obtain core-shells with semicontinuous gold shell, which are expected to have high extinction in broad spectral range. Interestingly, differences in optical properties were observed for TiO$_2$@Au structures. The significant red shift and broadening of the spectrum in the case of AuNPs decorated TiO$_2$ cores are likely related to high refractive index of TiO$_2$ and dense packing of AuNPs on TiO$_2$ particles surface, resulting in strong AuNPs plasmon-plasmon coupling. Modified Turkevich method yields core-shell nanostructures with dense surface and high reproducibility at temperatures in the 80–100 °C range. To the best of our knowledge, this is the first report describing the use of Turkevich method to direct fabrication of TiO$_2$@Au core-shell nanostructures.

Acknowledgments

Author Contributions

Bartłomiej J. Jankiewicz organized the research and wrote the manuscript; Paulina Dobrowolska, Aleksandra Krajewska and Magdalena Gajda-Rączka performed the experiments; Bartosz Bartosewicz and Piotr Nyga discussed the experiments and participated in writing manuscript. The manuscript was reviewed by all authors.

Conflicts of Interest

The authors declare no conflict of interest.

References

1. Rodriguez-Fernandez, J.; Perez-Juste, J.; Garcia de Abajo, F.J.; Liz-Marzan, L.M. Seeded growth of submicron Au colloids with quadrupole plasmon resonance rodes. *Langmuir* **2006**, *22*, 7007–7010.

2. Kim, F.; Sohn, K.; Wu, J.; Huang, J. Chemical synthesis of gold nanowires in acidic solutions. *J. Am. Chem. Soc.* **2008**, *130*, 14442–14443.

3. Jana, N.R.; Gearheart, L.; Murphy, C.J. Wet Chemical synthesis of silver nanorods and nanowires of controllable aspect ratio. *Chem. Commun.* **2001**, 617–618.

4. Jana, N.R.; Gearheart, L.; Murphy, C.J. Wet chemical synthesis of high aspect ratio gold nanorods. *J. Phys. Chem. B* **2001**, *105*, 4065–4067.

5. Vigderman, L.; Khanal, B.P.; Zubarev, E.R. Functional gold nanorods: Synthesis, self-assembly, and sensing applications. *Adv. Mater.* **2012**, *24*, 4811–4841.

6. Scarabelli, L.; Coronado-Puchau, M.; Giner-Casares, J.J.; Langer, J.; Liz-Marzán, L.M. Monodisperse gold nanotriangles: Size control, large-scale self-assembly, and performance in surface-enhanced raman scattering. *ACS Nano* **2014**, *8*, 5833–5842.

7. Kumar, P.S.; Pastoriza-Santos, I.; Rodriguez-Gonzalez, B.; Garcia de Abajo, F.J.; Liz-Marzan, L.M. High-yield synthesis and optical response of gold nanostars. *Nanotechnol.* **2008**, *19*, doi:10.1088/0957-4484/19/01/015606.

8. Jain, P.K.; Huang, X.; El-Sayed, I.H.; El-Sayed, M.A. Noble metals on the nanoscale: Optical and photothermal properties and some applications in imaging, sensing, biology, and medicine. *Acc. Chem. Res.* **2008**, *41*, 1578–1586.

9. Jain, P.K.; Lee, K.S.; El-Sayed, I.H.; El-Sayed, M.A. Calculated absorption and scattering properties of gold nanoparticles of different size, shape, and composition: Applications in biological imaging and biomedicine. *J. Phys. Chem. B* **2006**, *110*, 7238–7248.

10. Kelly, K.L.; Coronado, E.; Zhao, L.L.; Schatz, G.C. The optical properties of metal nanoparticles: The influence of size, shape, and dielectric environment. *J. Phys. Chem. B* **2003**, *107*, 668–677.

11. Oldenburg, S.J.; Averitt, R.D.; Westcott, S.L.; Halas, N.J. Nanoengineering of optical resonances. *Chem. Phys. Lett.* **1998**, *288*, 243–247.

12. Bardhan, R.; Lal, S.; Joshi, A.; Halas, N.J. Theranostic nanoshells: From probe design to imaging and treatment of cancer. *Acc. Chem. Res.* **2011**, *44*, 936–946.

13. Le, F.; Brandl, D.W.; Urzhumov, Y.A.; Wang, H.; Kundu, J.; Halas, N.J.; Aizpurua, J.; Nordlander, P. Metallic Nanoparticle arrays: A common substrate for both surface-enhanced raman scattering and surface-enhanced infrared absorption. *ACS Nano* **2008**, *2*, 707–718.

14. Bardhan, R.; Grady, N.K.; Cole, J.R.; Joshi, A.; Halas, N.J. Fluorescence enhancement by au nanostructures: Nanoshells and nanorods. *ACS Nano* **2009**, *3*, 744–752.

15. Neumann, O.; Ferontic, C.; Neumann, A.D.; Dong, A.; Schell, K.; Lue, B.; Kime, E.; Quinne, M.; Thompson, S.; Grady, N.; *et al*. Compact solar autoclave based on steam generation using broadband light-harvesting nanoparticles. *Proc. Natl. Acad. Sci. USA* **2013**, *110*, 11677–11681.

16. Jankiewicz, B.J.; Choma, J.; Jamioła, D.; Jaroniec, M. Silica-metal core-shell nanostructures. *Adv. Colloid Interface Sci.* **2012**, *170*, 28–47.

17. Antoschshuk, V.; Jaroniec, M. Adsorption, thermogravimetric, and nmr studies of fsm-16 material functionalized with alkylmonochlorosilanes. *J. Phys. Chem. B* **1999**, *103*, 6252–6261.

18. Xue, J.; Wang, C.; Ma, Z. A facile method to prepare a series of SiO_2@Au core/shell structured nanoparticles. *Mater. Chem. Phys.* **2007**, *105*, 419–425.

19. Ashayer, R.; Mannan, S.H.; Sajjadi, S. Synthesis and characterization of gold nanoshells using poly(diallyldimethyl ammonium chloride). *Colloids Surf. A* **2008**, *329*, 134–141.

20. Pham, T.; Jackson, J.B.; Halas, N.J.; Lee, T.R. Preparation and characterization of gold nanoshells coated with self-assembled monolayers. *Langmuir* **2002**, *18*, 4915–4920.

21. Preston, T.C.; Signorell, R. Growth and optical properties of gold nanoshells prior to the formation of a continuous metallic layer. *ACS Nano* **2009**, *3*, 3696–3706.

22. Kim, J.H.; Bryan, W.W.; Lee, T.R. Preparation, Characterization, and optical properties of gold, silver, and gold-silver alloy nanoshells having silica cores. *Langmuir* **2008**, *24*, 11147–11152.

23. Tharion, J.; Satija, J.; Mukherji, S. Glucose mediated synthesis of gold nanoshells: A facile and eco-friendly approach conferring high colloidal stability. *RSC Adv.* **2014**, *4*, 3984–3991.

24. Kim, J.H.; Bryan, W.W.; Chung, H.W.; Park, C.Y.; Jacobson, A.J.; Lee, T.R. Gold, palladium, and gold-palladium alloy nanoshells on silica nanoparticle cores. *ACS Appl. Mater. Interfaces* **2009**, *1*, 1063–1069.

25. Graf, C.; van Blaaderen, A. Metallodielectric colloidal core-shell particles for photonic applications. *Langmuir* **2002**, *18*, 524–534.

26. Brinson, B.E.; Lassiter, J.B.; Levin, C.S.; Bardhan, R.; Mirin, N.; Halas, N.J. Nanoshells made easy: Improving Au layer growth on nanoparticle surfaces. *Langmuir* **2008**, *24*, 14166–14171.

27. English, M.D.; Waclawik, E.R. A novel method for the synthesis of monodisperse gold-coated silica nanoparticles. *J. Nanopart. Res.* **2012**, *14*, 650–660.

28. Lim, Y.T.; Park, O.O.; Jung, H.T. Gold nanolayer-encapsulated silica particles synthesized by surface seeding and shell growing method: Near infrared responsive materials. *J. Colloid Interface Sci.* **2003**, *263*, 449–453.

29. Pol, V.G.; Gedanken, A.; Calderon-Moreno, J. Deposition of gold nanoparticles on silica spheres: A Sonochemical approach. *Chem. Mater.* **2003**, *15*, 1111–1118.

30. Choma, J.; Dziura, A.; Jamioła, D.; Nyga, P.; Jaroniec, M. Preparation and properties of silica-gold core-shell particles. *Colloids Surf. A* **2011**, *373*, 167–171.

31. Zhang, L.; Feng, Y.G.; Wang, L.Y.; Zhang, J.Y.; Chen, M.; Qian, D.J. Comparative studies between synthetic routes of SiO$_2$@Au composite nanoparticles. *Mater. Res. Bull.* **2007**, *42*, 1457–1467.

32. Storti, B.; Elisei, F.; Abbruzzetti, S.; Viappiani, C.; Latterini, L. One-pot synthesis of gold nanoshells with high photon-to-heat conversion efficiency. *J. Phys. Chem. C* **2009**, *113*, 7516–7521.

33. Zhang, P.; Guo, Y. Surface-enhanced raman scattering inside metal nanoshells. *J. Am. Chem. Soc.* **2009**, *131*, 3808–3809.

34. Turkevich, J.; Stevenson, P.L.; Hillier, J. A study of the nucleation and growth process in the synthesis of colloidal gold. *Discuss. Faraday Soc.* **1951**, *11*, 55–75.

35. Frens, G. Controlled nucleation for the regulation of the particle size in monodisperse gold suspensions. *Nature Phys. Sci.* **1973**, *241*, 20–22.

36. Westcott, S.L.; Oldenburg, S.J.; Lee, T.R.; Halas, N.J. Formation and adsorption of clusters of gold nanoparticles onto functionalized silica nanoparticle surfaces. *Langmuir* **1998**, *14*, 5396–5401.

37. Mueller, R.; Kammler, H.K.; Wegner, K.; Pratsinis, S.E. OH surface density of SiO$_2$ and TiO$_2$ by thermogravimetric analysis. *Langmuir* **2003**, *19*, 160–165.

38. Barabanova, A.I.; Pryakhina, T.A.; Afanas'ev, E.S.; Zavin, B.G.; Vygodskii, Y.S.; Askadskii, A.A.; Philippova, O.E.; Khokhlov, A.R. Anhydride modified silica nanoparticles: Preparation and characterization. *Appl. Surface Sci.* **2012**, *258*, 3168–3172.

39. Takahashi, J.; Itoh, H.; Motai, S.; Shimada, S. Dye adsorption behavior of anatase- and rutile-type TiO$_2$ nanoparticles modified by various heat-treatments. *J. Mater. Sci.* **2003**, *38*, 1695–1702.

40. De Silva, V.C.; Nyga, P.; Drachev, V.P. Scattering suppression of silica microspheres with semicontinuous plasmonic shell. *ArXiv E-Prints* **2015**, arXiv:1501.00233v1.

41. Rohde, C.A.; Hasegawa, K.; Deutsch, M. Coherent light scattering from semicontinuous silver nanoshells near the percolation threshold. *Phys. Rev. Lett.* **2006**, *96*, doi:10.1103/PhysRevLett. 96.045503.